PHYSICAL REVIEW B **78**, 134517 (2008)

Phase separation and collapse in Bose-Fermi mixtures with a Feshbach resonance

Francesca M. Marchetti*
Rudolf Peierls Centre for Theoretical Physics, University of Oxford, 1 Keble Road, Oxford OX1 3NP, United Kingdom

Charles J. M. Mathy and David A. Huse
Department of Physics, Princeton University, Princeton, New Jersey 08544, USA

Meera M. Parish†
Department of Physics, Princeton University, Princeton, New Jersey 08544, USA and Princeton Center for Theoretical Science, Princeton University, Princeton, New Jersey 08544, USA

(Received 4 January 2008; revised manuscript received 14 August 2008; published 14 October 2008)

We consider a mixture of single-component bosonic and fermionic atoms with an interspecies interaction that is varied using a Feshbach resonance. By performing a mean-field analysis of a two-channel model, which describes both narrow and broad Feshbach resonances, we find an unexpectedly rich phase diagram at zero temperature: Bose-condensed and non-Bose-condensed phases form a variety of phase-separated states that are accompanied by both critical and tricritical points. We discuss the implications of our results for the experimentally observed collapse of Bose-Fermi mixtures on the attractive side of the Feshbach resonance, and we make predictions for future experiments on Bose-Fermi mixtures close to a Feshbach resonance.

DOI: 10.1103/PhysRevB.78.134517 PACS number(s): 03.75.Ss, 64.60.Kw, 05.30.Jp, 03.75.Hh

I. INTRODUCTION

The possibility of controlling the interatomic interaction strength via Feshbach resonances has recently played a pivotal role in investigating condensation phenomena in ultracold alkali gases. A prominent example is the realization of condensed pairs in two-component Fermi gases, where one has a crossover from the weakly interacting BCS regime to a Bose-Einstein condensate (BEC) of diatomic molecules.[1,2] By tuning the two spin populations to be unequal, one can further explore quantum phase transitions and phase separation (see, e.g., Refs. 3 and 4 and references therein). Even richer scenarios are expected for heteronuclear resonances in Bose-Fermi mixtures because one can in principle destroy the BEC by binding bosons and fermions into *fermionic* molecules.[5] Moreover, a host of interesting phenomena has been predicted, such as spatial separation of bosons and fermions induced by interspecies repulsive interactions,[6,7] boson-mediated Cooper pairing,[8–10] density wave phases in optical lattices,[11] and the formation of polar molecules with dipolar interactions.

Following the recent detection of Feshbach resonances in Bose-Fermi mixtures,[12–15] experiments have begun to explore how the behavior of the ^{87}Rb-^{40}K system depends on the interspecies interaction strength.[16–20] Thus far, repulsive interactions (generated by approaching the resonance from the side of positive scattering length a_{BF}) have been observed to reduce the spatial overlap between fermions and the BEC. By contrast, attractive interactions can produce a sudden loss of atoms, which has been attributed to enhanced three-body recombination processes resulting from an unconstrained increase in the density. Current mean-field theories[6,21–23] predict that this *total* collapse of the mixture occurs above a critical density or interaction strength, where the mixture is dynamically unstable. However, these theories neglect any pairing between bosons and fermions, which we show plays a crucial role in the stability of the system.

In this paper, we address the possibility of pairing in Bose-Fermi mixtures by considering a two-channel model that explicitly includes fermionic molecules as an extra species of particle. Such a model encompasses both broad and narrow Feshbach resonances. We then determine the zero-temperature phase diagram for the Bose-Fermi mixture as a function of the interaction strengths and particle densities within a mean-field approximation. Sufficiently close to the resonance, we always find phase separation between a mixed BEC phase (where the BEC coexists with fermions) and either a pure BEC, mixed BEC, normal, or vacuum phase. This provides one of the few examples of phase separation in a Bose-Fermi mixture with *attractive* interactions—e.g., ^{3}He-^{4}He mixtures[24] and polarized Fermi gases[3,4] require effectively repulsive interactions. We explain why our results are consistent with the collapse observed in current experiments and we discuss the best conditions for observing the predicted phase separation.

The paper is organized as follows: Section II describes the two-channel model of a Bose-Fermi mixture and how it is related to the single-channel theory. In Sec. III, we derive the zero-temperature phase diagram of a homogeneous mixture. In Sec. IV we discuss its connection with current and future experiments and we then consider how the phase diagram will manifest itself in a trapped gas in Sec. IV A. We present our conclusions in Sec. V.

II. TWO-CHANNEL MODEL

We consider the two-channel Hamiltonian

$$\hat{H}_{2c} = \sum_{\mathbf{k}} (\xi^f_{\mathbf{k}} f^\dagger_{\mathbf{k}} f_{\mathbf{k}} + \xi^b_{\mathbf{k}} b^\dagger_{\mathbf{k}} b_{\mathbf{k}} + \xi^\psi_{\mathbf{k}} \psi^\dagger_{\mathbf{k}} \psi_{\mathbf{k}}) + \frac{g}{\sqrt{V}} \sum_{\mathbf{k},\mathbf{k}'} (\psi^\dagger_{\mathbf{k}+\mathbf{k}'} f_{\mathbf{k}} b_{\mathbf{k}'} + \text{H.c.}) + \frac{U_{\text{bg}}}{V} \sum_{\mathbf{k},\mathbf{k}',\mathbf{q}} b^\dagger_{\mathbf{k}} f^\dagger_{\mathbf{k}'} f_{\mathbf{k}'+\mathbf{q}} b_{\mathbf{k}-\mathbf{q}} + \frac{\lambda}{V} \sum_{\mathbf{k},\mathbf{k}',\mathbf{q}} b^\dagger_{\mathbf{k}} b^\dagger_{\mathbf{k}'} b_{\mathbf{k}'+\mathbf{q}} b_{\mathbf{k}-\mathbf{q}}, \tag{1}$$

which describes a mixture of bosonic b and fermionic f atoms coupled to a *fermionic* closed-channel molecule ψ via the interaction g, where V is the three-dimensional volume. Setting $\hbar=1$, the kinetic terms are given by

$$\xi^f_{\mathbf{k}} = \frac{\mathbf{k}^2}{2m_f} - \mu_f,$$

$$\xi^b_{\mathbf{k}} = \frac{\mathbf{k}^2}{2m_b} - \mu_b,$$

$$\xi^\psi_{\mathbf{k}} = \frac{\mathbf{k}^2}{2(m_b+m_f)} - \mu_f - \mu_b + \nu,$$

where ν is the detuning from resonance and μ_b (μ_f) is the chemical potential for the bosons (fermions). We also include the boson-boson interaction $\lambda = 2\pi a_{\text{bb}}/m_b$ and the background boson-fermion interaction $U_{\text{bg}} = 4\pi a_{\text{bg}}/m$, with $m = 2m_f m_b/(m_f+m_b)$. Clearly, we always require $\lambda > 0$ if we want the Bose gas to be stable.

A key energy scale in our model is the width of the resonance

$$\gamma = \frac{g^2}{8\pi} m^{3/2}, \quad \text{with } g = \sqrt{\frac{4\pi a_{\text{bg}} \Delta\mu \Delta B}{m}}, \tag{2}$$

where ΔB is the absolute width of the resonance in terms of the magnetic field and $\Delta\mu$ is the difference in magnetic moments between the closed and open channels (which is of order the Bohr magneton). When compared to the boson condensation temperature $k_B T_0 = 2\pi[n_b/g_{3/2}(1)]^{2/3}/m_b$ [with $g_{3/2}(1) \simeq 2.612$] and the Fermi energy $k_B T_F = (6\pi^2 n_f)^{2/3}/2m_f$, the width of the resonance defines both narrow $\gamma^2/k_B(T_0+T_F) \ll 1$ and wide $\gamma^2/k_B(T_0+T_F) \gg 1$ Feshbach resonances.

At zero temperature, the Hamiltonian (1) can be exactly diagonalized in the mean-field approximation $\langle b_{\mathbf{k}} \rangle = \delta_{\mathbf{k},0}\sqrt{V}\Phi$, implying that the two Fermi species dispersions ξ^f and ξ^ψ are now hybridized by the presence of the condensate

$$\xi^{F,\Psi} = \frac{1}{2}(\xi^f + U_{\text{bg}}\Phi^2 + \xi^\psi) \pm \frac{1}{2}\sqrt{(\xi^f + U_{\text{bg}}\Phi^2 - \xi^\psi)^2 + 4g^2\Phi^2}. \tag{3}$$

This leads to the following expression for the grand-canonical free-energy density $\Omega^{(0)}_{2c}(\mu_f,\mu_b) = \min_\Phi f_{2c}(\Phi;\mu_f,\mu_b)$:

$$f_{2c}(\Phi;\mu_f,\mu_b) = \frac{1}{V}\sum_{\mathbf{k}} [\Theta(-\xi^F_{\mathbf{k}})\xi^F_{\mathbf{k}} + \Theta(-\xi^\Psi_{\mathbf{k}})\xi^\Psi_{\mathbf{k}}] - \mu_b\Phi^2 + \lambda\Phi^4. \tag{4}$$

When $U_{\text{bg}} < 0$, the free energy is unbounded from below

$$f_{2c}(\Phi \to \infty;\mu_f,\mu_b) \propto -\Phi^5.$$

Therefore, a repulsive background interaction strength $U_{\text{bg}} > 0$ is required in order to have a stable solution. Later on, we will neglect U_{bg} in our calculations because, as we discuss in Sec. III, it will not affect the main features of the phase diagram provided it is sufficiently small.

Since experiments are performed at fixed densities, the chemical potentials μ_f and μ_b have to be determined from the total number of fermionic and bosonic atom densities

$$n_{f,b} = -\frac{\partial\Omega^{(0)}}{\partial\mu_{f,b}}. \tag{5}$$

Note that n_f (n_b) includes fermions (bosons) bound into molecules. Despite the simplicity of our approach, we emphasize that our mean-field analysis will be quantitatively accurate in the case of narrow Feshbach resonances[25] because Gaussian fluctuations beyond mean-field scale like $\gamma/\sqrt{k_B(T_0+T_F)}$. We also expect it to provide a qualitative description of the phase diagram for a broad Feshbach resonance as is the case in two-component Fermi gases—the phase diagram for polarized Fermi gases is qualitatively similar for broad and narrow Feshbach resonances.[26]

A. Connection to single-channel model

Before tackling the phase diagram, it is instructive to understand how our model connects with existing single-channel theories, where the closed-channel molecule ψ is ignored and we have Hamiltonian

$$\hat{H}_{1c} = \sum_{\mathbf{k}} (\xi^f_{\mathbf{k}} f^\dagger_{\mathbf{k}} f_{\mathbf{k}} + \xi^b_{\mathbf{k}} b^\dagger_{\mathbf{k}} b_{\mathbf{k}}) + \frac{1}{V}\sum_{\mathbf{k},\mathbf{k}',\mathbf{q}} (U_{\text{BF}} b^\dagger_{\mathbf{k}} f^\dagger_{\mathbf{k}'} f_{\mathbf{k}'+\mathbf{q}} b_{\mathbf{k}-\mathbf{q}} + \lambda b^\dagger_{\mathbf{k}} b^\dagger_{\mathbf{k}'} b_{\mathbf{k}'+\mathbf{q}} b_{\mathbf{k}-\mathbf{q}}), \tag{6}$$

with the effective Bose-Fermi interaction $U_{\text{BF}} = 4\pi a_{\text{BF}}/m$. Such a theory is expected to be appropriate for a broad Feshbach resonance, where there is only a small admixture of the closed-channel molecule, which can therefore be neglected. However, a mean-field analysis of the single-channel model focuses on densities only and does not take account of pairing correlations. Within this approximation, the system becomes linearly unstable when[7]

$$n_f^{1/3} \geq \frac{4}{3}\frac{(6\pi^2)^{2/3}}{2m_f}\frac{\lambda}{U^2_{\text{BF}}}. \tag{7}$$

For the case of attractive interactions $U_{\text{BF}} < 0$, one can easily show that the single-channel free energy is not bounded from below [$f_{1c}(\Phi\to\infty;\mu_f,\mu_b) \propto -\Phi^5$]. As a consequence, any state at finite density is metastable and, when Eq. (7) is satisfied, the system is unstable to a total collapse.[23] On the other hand, when $U_{\text{BF}} > 0$, the free energy is bounded and the instability is toward phase separation.

Now, we expect the two-channel model (1) to map to a single-channel Hamiltonian when we take the limit $\nu \to +\infty$, $g \to +\infty$ while holding $-g^2/\nu \equiv U_{\mathrm{BF}} < 0$ fixed because then the closed-channel molecule ψ effectively disappears from the problem while the scattering length a_{BF} is kept fixed. Indeed, we find that our two-channel mean-field theory (4) in the above limit is formally equivalent to the single-channel mean-field theory on the *attractive* side of the resonance with $U_{\mathrm{BF}} < 0$. Thus, in the low-density regime $(T_0 + T_F) \ll \gamma^2/k_B$ we expect the two-channel theory to reduce to the single-channel theory. Therefore, we expect to have linear instabilities and first-order transitions in the low-density region of the phase diagram. In addition, we do not expect our mean-field theory to include the pairing instabilities that have been shown to exist in the single-channel model,[27,28] although we speculate that the narrow Feshbach resonance limit may capture the qualitative features of these pairing correlations.

III. PHASE DIAGRAM

In the following, we will take the mass ratio to be $m_f/m_b \simeq 0.26$ as in ^{23}Na-^{6}Li mixtures because this atomic system has a narrow Feshbach resonance[12,29] and a small repulsive U_{bg}. Thus we are likely to observe experimentally the phase-separated states we predict here. While the behavior of ^{23}Na-^{6}Li mixtures is yet to be explored in detail, interspecies Feshbach resonances have already been identified experimentally. We emphasize that changing the mass ratio will only affect our results qualitatively and so our phase diagram will also be applicable to other atomic systems.

If one focuses on pairing only, it is clear that at the fixed density $n_f \geq n_b$ there is a transition as we cross the resonance: the BEC phase ($\Phi \neq 0$) will be completely depleted ($\Phi = 0$) by the binding of bosons into fermionic molecules. (Note that the formation of molecules can also involve a phase transition where the number of Fermi surfaces changes.) This transition was shown to be continuous for the limiting case of vanishing coupling $g = 0$.[30] Assuming the transition remains second order for $g \neq 0$, as in Ref. 5, the phase boundaries are found by solving $O(\Phi^2) \equiv \partial f_{2c}/\partial \Phi^2|_{\Phi=0} = 0$. However, as we anticipated in Sec. II A, in general we find that there can also be first-order transitions between two BEC phases as well as between BEC and normal (N) phases. Before we explain the main features of the phase diagram, it is useful to examine how the second-order transition becomes first order.

Precursors of first-order transitions can be found in tricritical points, where $O(\Phi^2) = 0$ and $O(\Phi^4) \equiv \partial^2 f_{2c}/\partial(\Phi^2)^2|_{\Phi=0} = 0$. Surprisingly, the mean-field energy $f_{2c}(\Phi; \mu_f, \mu_b)$ can be expressed in terms of just three independent dimensionless parameters, and thus the phase transitions can be completely characterized by the dimensionless parameters

$$\{\mu_f^{(r)}, \nu^{(r)}, \mu_b^{(r)}\} = c^{1/3}\left\{c^{1/3}\frac{\mu_f}{\gamma^2}, c^{1/3}\frac{\nu - \mu_b}{\gamma^2}, \frac{\mu_b}{\gamma^2}\right\}, \qquad (8)$$

where $c = \lambda m_b^{2/3}\gamma$. Referring to Fig. 1, in these units we find that for $|\nu^{(r)}|$ greater than the tetracritical values at which $O(\Phi^2) = O(\Phi^4) = O(\Phi^6) = 0$ (open circles), there are lines of

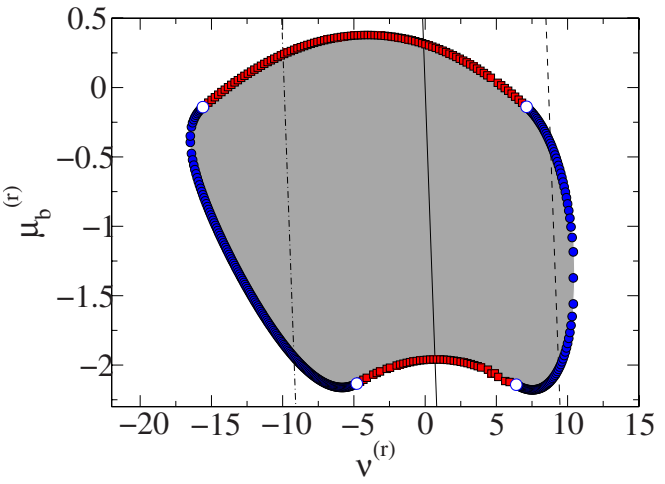

FIG. 1. (Color online) Surface of first-order phase transitions in the three-dimensional (3D) space $\{\mu_f^{(r)}, \nu^{(r)}, \mu_b^{(r)}\} \equiv c^{1/3}\{c^{1/3}\mu_f/\gamma^2, c^{1/3}(\nu - \mu_b)/\gamma^2, \mu_b/\gamma^2\}$, where $c = \lambda m_b^{2/3}\gamma$, that has been projected onto the $(\nu^{(r)}, \mu_b^{(r)})$ plane. The gray shaded area corresponds to the first-order region. For $|\nu^{(r)}|$ greater than the tetracritical points $O(\Phi^2) = O(\Phi^4) = O(\Phi^6) = 0$ (open circles), we have lines of tricritical points represented by the (blue) filled circles. Otherwise, they are replaced by critical points [(red) filled squares]. The straight lines correspond to the cuts at fixed ν/γ^2 and c in Fig. 2, where we have $c \simeq 0.044$ and $\nu/\gamma^2 = -80$ (dotted-dashed), 0 (solid), and 70 (dashed) going from left to right.

tricritical points [(blue) filled circles] where the transition changes from second to first order. Beyond the tetracritical points, the tricritical points are replaced by critical points [(red) filled squares]. At a critical point two equal-energy minima of $f_{2c}(\Phi; \mu_f, \mu_b)$ merge. In this case, an expansion in Φ^2 cannot be exploited any longer. However, this failure of the expansion is not so surprising because, when $\lambda = 0$, the mean-field potential (4) is unbounded from below [$f_{2c}(\Phi \to \infty; \mu_f, \mu_b) \propto -\Phi^{5/2}$]. This nonanalytic dependence on Φ comes from the hybridized Fermi dispersions $\xi^{F,\Psi}$.

Therefore, to summarize, we find that the first-order regime is confined by either tricritical or critical points within a region about the origin of the $\{\mu_f^{(r)}, \nu^{(r)}, \mu_b^{(r)}\}$ parameter space. Outside of this region, we only find continuous transitions. From the definition of $\{\mu_f^{(r)}, \nu^{(r)}, \mu_b^{(r)}\}$, one can see that the ratio $\lambda m_b^{3/2}/\gamma^2$ sets the energy scale of the problem and determines the chemical potentials at which the tricritical points are replaced by critical points in Fig. 1. As explained above, one expects first-order transitions to appear in the limit $\lambda \to 0$. However, note also that one can access the regime of first-order transitions even when the repulsion between bosons λ is large by making μ_f, ν, and μ_b sufficiently small—as a consequence we expect these results to apply in the low-density limit close to resonance. We have checked that a small repulsive background interaction U_{bg} only brings small quantitative changes to this result by slightly reducing the size of the first-order region.

While one can parameterize the entire phase diagram using the rescaled parameters $\{\mu_f^{(r)}, \nu^{(r)}, \mu_b^{(r)}\}$, from the point of view of real systems, it makes more sense to consider the parameters $\{c \equiv \lambda m_b^{3/2}\gamma, \nu/\gamma^2, \mu_b/\gamma^2, \mu_f/\gamma^2\}$. For a given experiment, c is fixed by the typical boson-boson interaction

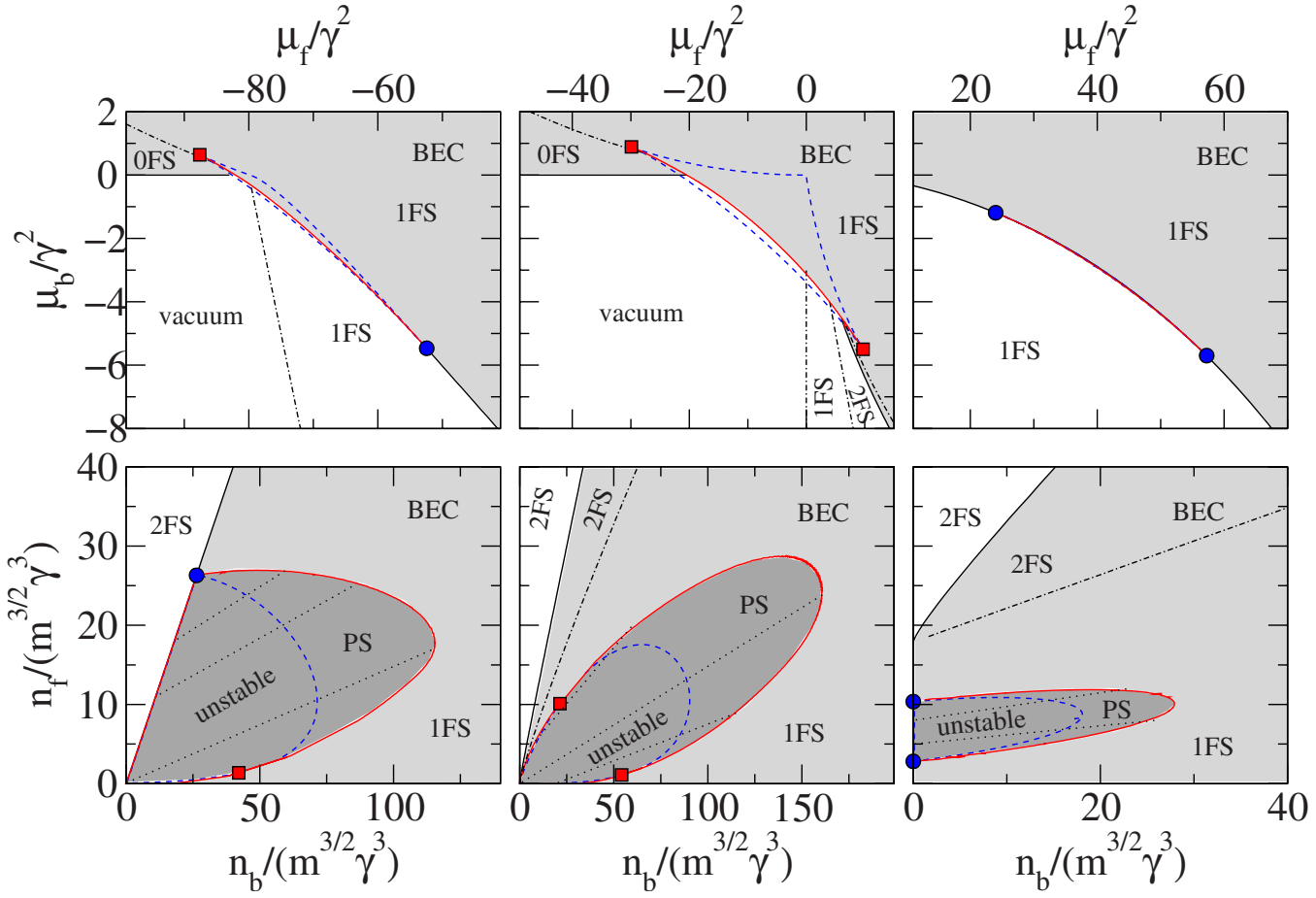

FIG. 2. (Color online) Zero-temperature mean-field phase diagrams for ^{23}Na-^{6}Li mixtures, where $c=\lambda m_b^{3/2}\gamma\simeq 0.044$. The top and bottom rows correspond to chemical potential and density space, respectively, while the columns represent different detunings: $\nu/\gamma^2=-80$ ($a_{\mathrm{BF}}\simeq -475a_0$), $\nu/\gamma^2=0$, and $\nu/\gamma^2=70$ ($a_{\mathrm{BF}}\simeq 543a_0$), going from left to right. The various phases can be distinguished based on the number of Fermi surfaces and whether or not there is a BEC (light gray shaded region). The solid thick (red) lines represent first-order phase transitions, which are accompanied by regions of phase separation (dark gray shaded region) in density space, while the thin solid (black) lines of the phase boundaries are continuous. The dotted-dashed lines separate regions with a different number of Fermi surfaces. The dotted lines that connect points on the first-order boundary depict which phases constitute the phase-separated state at a given density. A filled (blue) circle denotes a tricritical point, a filled (red) square denotes a critical point, and a dashed (blue) line denotes a spinodal line.

strength and width of the resonance, while ν/γ^2 is determined by the Bose-Fermi scattering length $a_{\mathrm{BF}}=-2\gamma/\sqrt{m\nu}$. Therefore, the phase diagram can be plotted as a function of the chemical potentials (top row of Fig. 2). These slices correspond to planes in Fig. 1 given by $\mu_b^{(r)}=-\nu^{(r)}/c^{1/3}+c^{1/3}\nu/\gamma^2$. In order to be relevant to experiments on ^{23}Na-^{6}Li mixtures, we use the scattering lengths $a_{\mathrm{bg}}=13.0a_0$ and $a_{\mathrm{bb}}=85a_0$, where a_0 is the Bohr radius, and take the resonance width to be $\Delta B=2.2$G.[29] For these values of the parameters, we have $c\simeq 0.044$ and $a_{\mathrm{BF}}=-3.8\times 10^4 a_0\gamma^2/\nu$. However, the qualitative behavior of the phase diagram as depicted in Fig. 2 will apply for all $c\lesssim 25$. In this regime, first-order transitions appear only in the finite interval around unitarity $c^{2/3}\nu/\gamma^2\in[-18,11]$. At the resonance, we find two critical points (and two accompanying critical end points, where first and second-order transitions meet), while moving far from the resonance in either direction, first one and then both critical points are replaced by tricritical points until eventually for large enough detuning the first-order transition region disappears altogether.

In terms of the phase diagram in density space (bottom row of Fig. 2), first-order transitions imply phase separation (PS) between BEC and N (BEC and BEC) close to a tricritical (critical) point. Here, N satisfies $n_f=n_b$ when $\nu<0$ and $n_b=0$ when $\nu>0$. Both BEC and N phases can be further characterized by the number of Fermi surfaces (FS). In the N region, the second-order boundaries between regions with different numbers of FS are defined by $\mu_f=0$ ($n_b=n_f$) and $\mu_b=-\mu_f+\nu$ ($n_b=0$). In the BEC phase instead one has to impose the condition $g^2\Phi^2=\mu_f(\mu_f+\mu_b-\nu)$. A special case of PS occurs when the N phase is the vacuum. Physically this is equivalent to a *partial* collapse of the system to higher densities. On the attractive side of the resonance $\nu>0$ and for small enough densities $(T_0+T_F)\ll\gamma^2/k_B$, we expect to recover the results of the single-channel theory. In particular, close enough to the resonance and for small enough densities, the condition for linear instability becomes independent of the boson density resembling Eq. (7).

At this point, a question that naturally arises is why does one observe phase separation instead of the *total* collapse

predicted by the single-channel mean-field theory. The answer is that the presence of closed-channel fermionic molecules stabilizes the large Φ behavior and constrains unbounded increases in density, converting the total collapse into phase separation. One can intuitively understand this as follows: once the Bose-Fermi mixture becomes unstable, the resulting increase in density will likewise increase the population of (virtual) closed-channel fermionic molecules, which in turn will exert an increasing Fermi pressure. Eventually, this Fermi pressure will balance the negative pressure of the attractive interactions so that the gas becomes stable at a finite density. This scenario is perhaps most clearly illustrated close to unitarity, where phase separation takes the form of a partial collapse.

Within the PS region it is possible to distinguish a metastable and an unstable (or spinodal) region separated by a spinodal line, where minimum and maximum of $f_{2c}(\Phi;\mu_f,\mu_b)$ merge. Inside the spinodal region, the dynamics of phase separation following a sudden quench proceeds via a linear instability (see, e.g., Ref. 31 and references therein), while it is characterized by nucleation in the metastable region. A calculation of the spinodal lines has also been carried out in Ref. 5 at a fixed n_b, although the possibility of phase separation was not considered.

In addition, Ref. 5 suggests that, when $n_f < n_b$, there is a smooth crossover at fixed density from the atomic to the molecular side of the resonance within the same BEC-1FS phase. We find that this crossover exists for sufficiently large densities, while phase separation intervenes at smaller densities $n_f \lesssim 30m^{3/2}\gamma^3$ and $n_b \lesssim 170m^{3/2}\gamma^3$ (Fig. 2). More generally, the size of the phase-separated region scales like γ^2/λ for both n_f and the molecular component of n_b, while the condensed component of n_b scales like $\gamma^2/(\lambda c^{1/3})$.

Finally, we note that the narrow Feshbach resonance regime $\gamma^2/k_B(T_0+T_F) < 1$ corresponds to densities $n_f > 0.02m^{3/2}\gamma^3$ or $n_b > 0.6m^{3/2}\gamma^3$, therefore our mean-field treatment should be reasonable for the region of interest. Certainly, the unstable region is a robust feature of the overall phase diagram because we can arbitrarily increase the size of it in density space by decreasing λ/γ^2 or $\lambda c^{1/3}/\gamma^2$.

IV. IMPLICATIONS FOR EXPERIMENT

The existence of three-body recombination in Bose-Fermi mixtures poses a major challenge to investigating experimentally the phase diagram we have described in Sec. III. In current experiments on ^{87}Rb-^{40}K mixtures, the behavior of the mixture is dominated by the large attractive background interaction—one even achieves collapse far from the resonance by increasing the density.[16–18] Even if one ignores the background scattering length, we find that the phase-separated states close to resonance, as in Fig. 2, evaluated for the parameters of ^{87}Rb-^{40}K, involve such a large increase in density (becoming of order 10^{16} cm^{-3} or more) that they will be destroyed by three-body recombination. Thus, we do not expect experiments on ^{87}Rb-^{40}K mixtures to reveal the rich variety of phase-separated states we have predicted. On the other hand, a density of 10^{12} cm^{-3} in ^{23}Na-^{6}Li mixtures corresponds to $n_b/m^{3/2}\gamma^3 \sim 1$ and so the phase-separated state possesses densities in the range of $10^{13}-10^{14}$ cm^{-3}, which should be easily accessible experimentally.

The dominant three-body process involves one fermionic atom and two bosonic atoms, with recombination rate $\Gamma \propto a_{\mathrm{BF}}^4 n_f n_b^2$ away from resonance.[32] Thus, to minimize Γ in the phase-separated state, we must reduce the densities and/or $|a_{\mathrm{BF}}|$ at which phase separation first appears. Assuming the bosons are mostly condensed and using the scalings de-

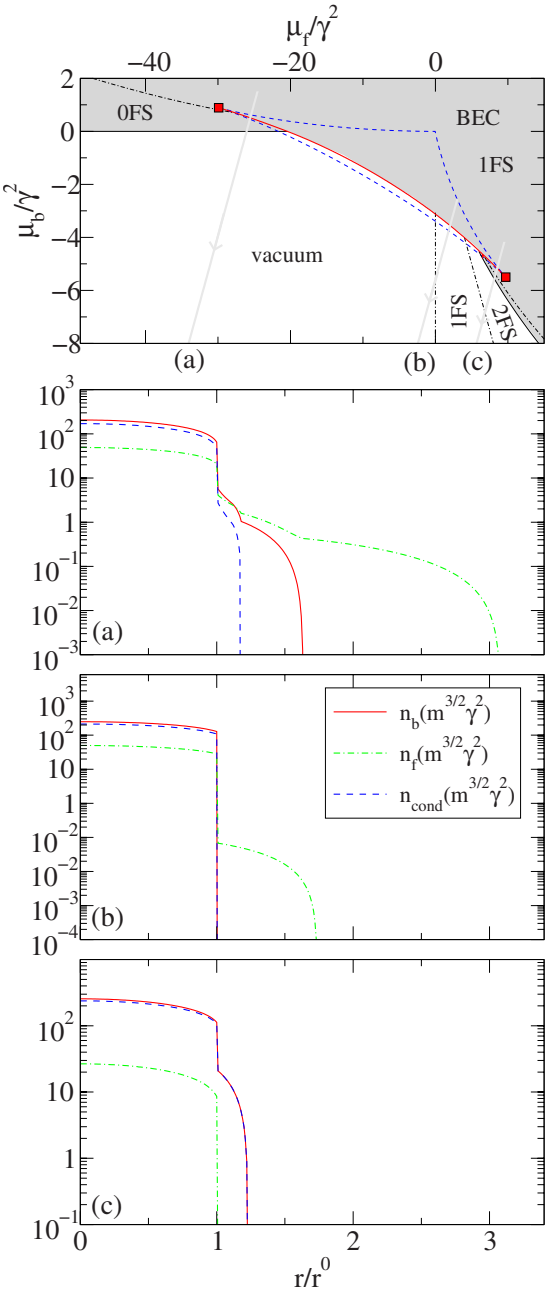

FIG. 3. (Color online) Trap density profiles at $\nu=0$ for boson number n_b, fermion number n_f, and condensed boson number $n_{\mathrm{cond}} \equiv \Phi^2/g^2$ in units of $m^{3/2}\gamma^3$, where $\lambda m_b^{3/2}\gamma \simeq 0.044$. The profiles correspond to three different cuts (a), (b), and (c) across the chemical-potential phase diagram as shown in the top panel, where the gray arrows represent trajectories from the center to the edge of the trap. In all three cases $r=r_0$ has been fixed as the point at which the first-order transition occurs.

scribed previously, we get $\Gamma/n_b \propto m^{3/2}\lambda^{1/3}\gamma^{7/8}$ and $\Gamma/n_f \propto m\gamma^2$. Therefore, we must consider small γ, such as the Feshbach resonance for ^{23}Na-^{6}Li mixtures,[12] and perhaps small λ, although the dependence of Γ on λ is sensitive to the precise power of $|a_{\mathrm{BF}}|$, which in turn can depend on the width of the resonance.[33] One might also worry about three-body losses resulting from collisions between the closed-channel molecule ψ and the open-channel atoms. However, we point out that the "bare" molecule-atom interaction is generally unrelated to the resonance-induced interaction in the open channel and is, thus, generally negligible. Therefore, any collisions between closed-channel molecules and atoms will have to be due to effective interactions resulting from higher-order processes that involve multiple scattering among the atoms in the open channel. Such processes on the attractive side of the resonance should already be encompassed by our analysis of three-body collisions above.

On the repulsive side of the resonance $U_{\mathrm{BF}}>0$, the mean-field single-channel theory predicts phase separation between atomic bosons and fermions induced by the repulsion.[7] One can instead access the regime of model (1) by starting from $a_{\mathrm{BF}}<0$ and sweeping through the resonance to the molecular side $a_{\mathrm{BF}}>0$. Indeed, while most of the experiments have focused on the repulsive Bose-Fermi interaction, fermionic molecules have been very recently produced.[19,20,34] However, these studies currently paint a pessimistic picture of the stability of these *real* (as opposed to virtual closed-channel) molecules with respect to three-body recombination.

A. Trapped gases

In principle, one can detect phase separation using *in situ* absorption measurements. To extract the behavior of the trapped gas from the uniform phase diagram (Fig. 2), we use the local-density approximation to convert the effects of the trap into spatially varying chemical potentials. As shown in Fig. 3, the spatial trajectory in a trap is then represented by the straight line $\mu_{f,b}(\mathbf{r})/\gamma^2=\mu_{f,b}(0)/\gamma^2-V(\mathbf{r})/\gamma^2$ in the phase diagram, assuming that the fermionic and bosonic atoms experience the same harmonic trapping potential $V(\mathbf{r})$.[18] Phase separation in a trap occurs when the first-order boundary between BEC and N is crossed, yielding a discontinuity in the density profiles. In this case, the central phase is always a BEC (with 1FS), while the surrounding phases can be either BEC or N (with different numbers of FS). In particular, the partially collapsed gas will exhibit a sharp interface with the vacuum. The presence of density discontinuities will provide the primary signature for the phase separation predicted here.

V. CONCLUSION

In conclusion, we have analyzed the zero-temperature phase diagram for a Bose-Fermi mixture with an interaction strength tunable via a Feshbach resonance. By making use of a two-channel model, we have found a finite region of phase separation around resonance that is bounded by either tricritical or critical points. Close to unitarity, phase separation takes the form of a *partial* collapse of the system, where phase separation occurs between a higher density mixed BEC phase (BEC coexisting with either atomic or molecular fermions) and the vacuum. Such a sudden increase in density implies a larger three-body recombination, and thus our phase-separated states may be a challenge to realize experimentally. Indeed, current experiments on ^{87}Rb-^{40}K mixtures are dominated by total collapse in the case of attractive interactions.[16–18] However, we have argued that mixtures with a small resonance width and a small repulsive background interaction, such as ^{23}Na-^{6}Li mixtures,[12] stand a better chance of realizing the phase diagram we predict.

Finally, we note that in this work we have neglected the possibility of fermionic superfluidity induced by density fluctuations of the bosonic condensate. For a spin polarized Fermi gas, boson-mediated *p*-wave[9] and *s*-wave odd-frequency[10] Cooper pairings have been recently analyzed for the single-channel model. In both cases it has been found that the conditions for Cooper pairing are favorable for a repulsive enough Bose-Fermi interaction strength U_{BF}. However, at least for ^{23}Na-^{6}Li mixtures, we expect these phases to occur at densities much larger than the ones considered in the phase diagram of Fig. 2.

ACKNOWLEDGMENTS

We are grateful to J. Chalker, V. Gurarie, P. B. Littlewood, and G. Modugno for stimulating discussions. F.M.M. would like to acknowledge the financial support of the EPSRC-GB. This research was supported in part by the National Science Foundation under Grants No. PHY05-51164, No. DMR-0645461, and No. DMR-0213706.

*fmm25@cam.ac.uk
†mparish@princeton.edu

[1] C. A. Regal, M. Greiner, and D. S. Jin, Phys. Rev. Lett. **92**, 040403 (2004).
[2] M. W. Zwierlein, C. A. Stan, C. H. Schunck, S. M. F. Raupach, A. J. Kerman, and W. Ketterle, Phys. Rev. Lett. **92**, 120403 (2004).
[3] Y. Shin, M. W. Zwierlein, C. H. Schunck, A. Schirotzek, and W. Ketterle, Phys. Rev. Lett. **97**, 030401 (2006).
[4] G. B. Partridge, W. Li, Y. A. Liao, R. G. Hulet, M. Haque, and H. T. C. Stoof, Phys. Rev. Lett. **97**, 190407 (2006).
[5] S. Powell, S. Sachdev, and H. P. Büchler, Phys. Rev. B **72**, 024534 (2005).
[6] K. Mølmer, Phys. Rev. Lett. **80**, 1804 (1998).
[7] L. Viverit, C. J. Pethick, and H. Smith, Phys. Rev. A **61**, 053605 (2000).
[8] H. Heiselberg, C. J. Pethick, H. Smith, and L. Viverit, Phys. Rev. Lett. **85**, 2418 (2000).
[9] K. Suzuki, T. Miyakawa, and T. Suzuki, Phys. Rev. A **77**, 043629 (2008).

[10] R. M. Kalas, A. V. Balatsky, and D. Mozyrsky, arXiv:0806.0419 (unpublished).
[11] M. Lewenstein, L. Santos, M. A. Baranov, and H. Fehrmann, Phys. Rev. Lett. **92**, 050401 (2004).
[12] C. A. Stan, M. W. Zwierlein, C. H. Schunck, S. M. F. Raupach, and W. Ketterle, Phys. Rev. Lett. **93**, 143001 (2004).
[13] S. Inouye, J. Goldwin, M. L. Olsen, C. Ticknor, J. L. Bohn, and D. S. Jin, Phys. Rev. Lett. **93**, 183201 (2004).
[14] F. Ferlaino, C. D'Errico, G. Roati, M. Zaccanti, M. Inguscio, G. Modugno, and A. Simoni, Phys. Rev. A **73**, 040702(R) (2006).
[15] B. Deh, C. Marzok, C. Zimmermann, and P. W. Courteille, Phys. Rev. A **77**, 010701(R) (2008).
[16] C. Ospelkaus, S. Ospelkaus, K. Sengstock, and K. Bongs, Phys. Rev. Lett. **96**, 020401 (2006).
[17] S. Ospelkaus, C. Ospelkaus, L. Humbert, K. Sengstock, and K. Bongs, Phys. Rev. Lett. **97**, 120403 (2006).
[18] M. Zaccanti, C. D'Errico, F. Ferlaino, G. Roati, M. Inguscio, and G. Modugno, Phys. Rev. A **74**, 041605(R) (2006).
[19] G. Modugno, arXiv:cond-mat/0702277 (unpublished).
[20] J. J. Zirbel, K.-K. Ni, S. Ospelkaus, J. P. D'Incao, C. E. Wieman, J. Ye, and D. S. Jin, Phys. Rev. Lett. **100**, 143201 (2008).
[21] S. K. Adhikari, Phys. Rev. A **70**, 043617 (2004).
[22] M. Modugno, F. Ferlaino, F. Riboli, G. Roati, G. Modugno, and M. Inguscio, Phys. Rev. A **68**, 043626 (2003).
[23] S. T. Chui, V. N. Ryzhov, and E. E. Tareyeva, JETP Lett. **80**, 274 (2004).
[24] E. H. Graf, D. M. Lee, and J. D. Reppy, Phys. Rev. Lett. **19**, 417 (1967).
[25] A. V. Andreev, V. Gurarie, and L. Radzihovsky, Phys. Rev. Lett. **93**, 130402 (2004).
[26] M. M. Parish, F. M. Marchetti, A. Lamacraft, and B. D. Simons, Nat. Phys. **3**, 124 (2007).
[27] M. Y. Kagan, I. V. Brodsky, D. V. Efremov, and A. V. Klaptsov, Phys. Rev. A **70**, 023607 (2004).
[28] A. Storozhenko, P. Schuck, T. Suzuki, H. Yabu, and J. Dukelsky, Phys. Rev. A **71**, 063617 (2005).
[29] M. Gacesa, P. Pellegrini, and R. Côté, Phys. Rev. A **78**, 010701(R) (2008).
[30] H. Yabu, Y. Takayama, and T. Suzuki, Physica B (Amsterdam) **329-333**, 25 (2003).
[31] A. Lamacraft and F. M. Marchetti, Phys. Rev. B **77**, 014511 (2008).
[32] J. P. D'Incao and B. D. Esry, Phys. Rev. Lett. **94**, 213201 (2005).
[33] D. S. Petrov, Phys. Rev. Lett. **93**, 143201 (2004).
[34] C. Ospelkaus, S. Ospelkaus, L. Humbert, P. Ernst, K. Sengstock, and K. Bongs, Phys. Rev. Lett. **97**, 120402 (2006).